

Zn-Polyacrylate Tentacles in Microporous Organic Polymers as Nanocatalysts for Polycaprolactone Synthesis

Jong Doo Lee, Yoon-Joo Ko, Sang Moon Lee, Hae Jin Kim, and Seung Uk Son*

Cite This: <https://doi.org/10.1021/acsnm.2c03480>

Read Online

ACCESS |

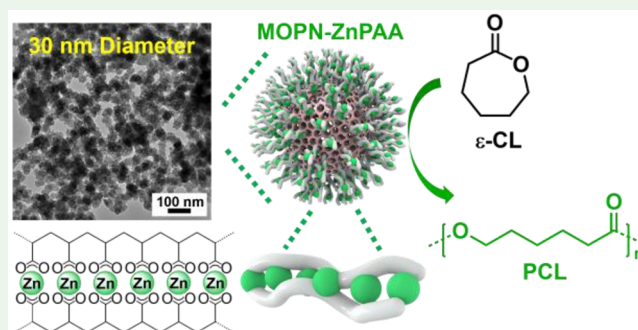
Metrics & More

Article Recommendations

Supporting Information

ABSTRACT: This work suggests an in situ synthetic approach for nanoplatfoms based on microporous organic polymer (MOP) chemistry. Anchoring groups for catalytic species could be simultaneously introduced to nanoplatfoms in the synthesis of MOPs. Poly(acrylic acid) (PAA) served not only as a surfactant for the controlled synthesis of nanoscaled MOPs but also as an anchoring group for the introduction of catalytic species. Zinc ions could be coordinated to MOP nanoparticles bearing PAA (MOPN-PAA) to form MOPN bearing ZnPAA (MOPN-ZnPAA). The MOPN-ZnPAA was well dispersed in neat ϵ -caprolactone (ϵ -CL) and showed excellent catalytic activities in the ring-opening polymerization of ϵ -CL to polycaprolactone (PCL). In addition, the MOPN-ZnPAA could be recycled, maintaining catalytic performance in five successive reactions.

KEYWORDS: nanocatalyst, microporous organic polymer, zinc catalyst, heterogeneous catalyst, polycaprolactone



During the last two decades, there has been great progress in the size-controlled engineering of nanomaterials.¹ The basic features of nanomaterials such as a high surface area and good dispersion ability are beneficial for their functional performance, compared with conventional bulky systems.¹ In this regard, nanoscaled catalysts have been extensively developed as new heterogeneous catalytic systems for various organic transformations.² While metallic nanoparticles could be directly utilized as catalysts, the designed catalytic species could also be incorporated into nanoscaled materials.² In the conventional stepwise synthesis of heterogeneous nanocatalysts bearing designed catalytic species, nanoscaled platfoms are first prepared and then the anchoring groups are introduced into nanoplatfoms (Figure 1a).³ If the designed

anchoring groups can be in situ introduced into nanoplatfoms during the synthesis of solid supports, the synthesis will become more expedient (Figure 1b). However, this kind of in situ approach was rarely explored.^{4,5}

Microporous organic polymers (MOPs) are versatile materials with high surface areas, microporosity, and chemical stability.⁶ Recently, various MOPs have been prepared by the networking of rigid building blocks.⁶ We speculated that the conventional synthetic chemistry of MOPs can be applied for the in situ engineering of nanoscaled platfoms bearing the designed anchoring groups. Various commercial polymers with functional groups can be utilized as surfactants for the size-controlled synthesis of MOPs, leading to the kinetically hindered growth of MOPs. During the growth process of MOPs, the polymers with functional groups can be in situ entrapped into the networks of MOPs⁷ and finally can be utilized as anchoring groups for targeted catalytic species. Ultimately, new heterogeneous nanocatalysts bearing the designed catalytic species can be realized based on MOP chemistry.

Recently, Zn-based catalysts have attracted significant attention from scientists.⁸ Because zinc is a relatively less

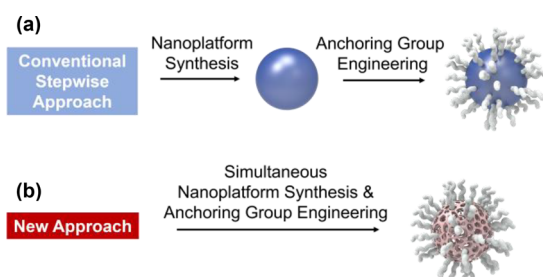


Figure 1. Comparison of synthetic approaches for nanocatalysts: (a) Conventional stepwise approach for nanoplatfoms with anchoring groups. (b) In situ approach for nanoplatfoms bearing anchoring groups.

Received: August 7, 2022

Accepted: August 19, 2022

toxic metal,⁹ zinc-based materials have been applied as Lewis acid catalysts in the synthesis of environmental-friendly materials.^{10–13} For example, Zn-glutarate has been applied as a catalyst for the synthesis of polycarbonates.¹⁴ In addition, Zn-based catalysts can be used in the ring-opening polymerization of ϵ -caprolactone (ϵ -CL) to biodegradable polycaprolactone (PCL).^{15–19} However, Zn-based heterogeneous catalysts have been relatively less explored.^{15–19} We have found that zinc ions can be easily loaded on poly(acrylic acid) (PAA) to form zinc polyacrylates (ZnPAA).²⁰ The ZnPAA can be utilized as a Lewis acid catalyst in the ring-opening polymerization of ϵ -CL. Unfortunately, the ZnPAA catalyst could not be recycled due to a chain structure-induced soluble feature. Thus, we have tried to engineer nanoscaled heterogeneous catalysts bearing ZnPAA.

In this work, we report the engineering of MOP nanoparticles bearing PAA (MOPN-PAA), the synthesis of heterogeneous nanocatalysts bearing ZnPAA (MOPN-ZnPAA), and their catalytic performance in the ring-opening polymerization of ϵ -CL to PCL.

Figure 2 shows a synthetic scheme for MOPN-PAA and MOPN-ZnPAA.

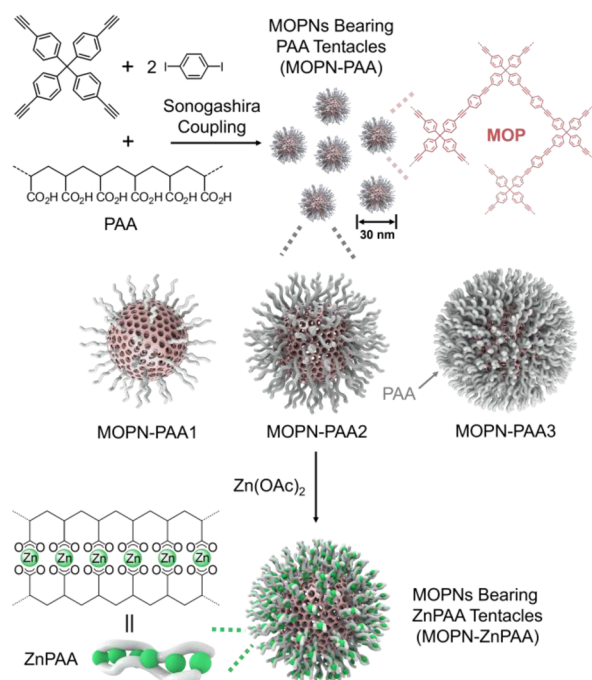


Figure 2. Synthesis of microporous organic polymer nanoparticles bearing PAA tentacles (MOPN-PAA) and MOPN-ZnPAA using MOPN-PAA2.

The Sonogashira coupling of tetra(4-ethynylphenyl)methane with 1,4-diiodobenzene in the presence of PAA resulted in the entrapment of PAA into the network to form MOPN-PAA. With a fixed amount (0.24 mmol) of tetra(4-ethynylphenyl)methane, the amount of PAA was increased from 0 to 20, 100, and 300 mg to form MOP, MOPN-PAA1, MOPN-PAA2, and MOPN-PAA3, respectively (refer to the Experimental Section for the MOPN-PAA prepared using 150–250 mg of PAA). Zinc ions were incorporated into MOPN-PAA2 through a reaction with zinc acetate to form MOPN-ZnPAA. A control material, ZnPAA was prepared by the reaction of PAA with zinc acetate.

The morphologies of MOP, MOPN-PAA, MOPN-ZnPAA, and ZnPAA were investigated by scanning (SEM) and transmission electron microscopy (TEM) (Figure 3). When

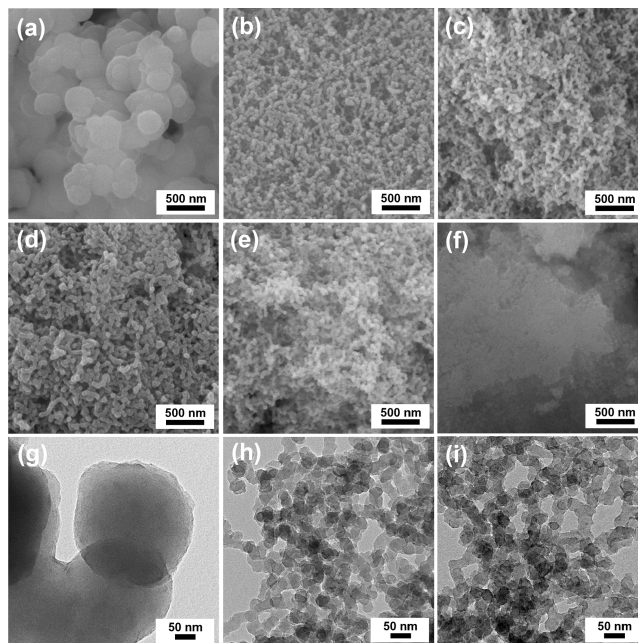


Figure 3. SEM images of (a) MOP, (b) MOPN-PAA1, (c) MOPN-PAA2, (d) MOPN-PAA3, (e) MOPN-ZnPAA, and (f) ZnPAA. TEM images of (g) MOP, (h) MOPN-PAA2, and (i) MOPN-ZnPAA.

the MOP was prepared without PAA, conventional MOP particles with diameters of 330–450 nm were formed (Figure 3a, g and Figure S1). In comparison, MOPN-PAA1 and MOPN-PAA2 showed uniform nanoparticles with an average size of 30 nm, due to the kinetically controlled growth of MOP (Figures 3b, c, h, and Figure S1).^{1,21–25} The sizes of MOPN-PAA3 increased to ~45 nm (Figure 3d), resulting from the generation of fewer nuclei in the early stage of MOP formation,¹ compared with the cases of MOPN-PAA1–2. Moreover, MOPN-PAA3 particles were significantly attached to one another, due to the excess PAA (Figure S3). Thus, we selected MOPN-PAA2 as an optimal nanoplatform to incorporate zinc ions (refer to the Experimental Section for the results of MOPN-PAA3 as a nanoplatform to incorporate zinc ions). The size of MOPN-PAA2 was retained in the MOPN-ZnPAA (Figures 3e, i, and Figure S1). In comparison, ZnPAA showed aggregated materials (Figure 3f and Figure S1).

To characterize the porosity and surface areas of materials, we obtained N₂ adsorption–desorption isotherm curves at 77 K and analyzed based on the Brunauer–Emmett–Teller (BET) theory (Figure 4 and Table S1). The MOP prepared without PAA showed a surface area of 470 m²/g and microporosity (micropore volume, V_{mic}: 0.14 cm³/g) (Figure 4a, b). Interestingly, the surface area and V_{mic} of MOPN-PAA1 increased to 807 m²/g and 0.19 cm³/g, respectively (Figures 4a, b). It has been reported that the MOPs prepared by the Sonogashira coupling of building blocks are amorphous materials.⁶ In our study, powder X-ray diffraction (PXRD) studies showed that MOP, MOPN-PAA, and MOPN-ZnPAA are amorphous materials (Figure S2). This implies that the network structures of MOPs contain incomplete networks,

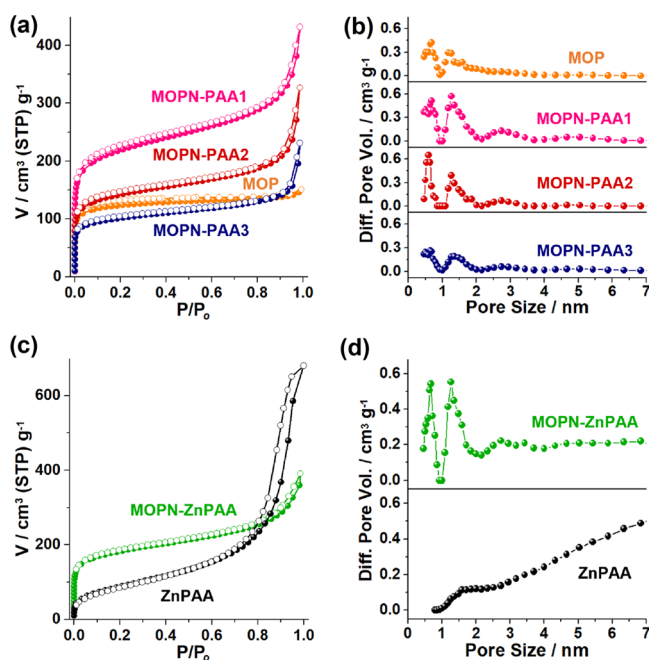


Figure 4. (a, c) N_2 adsorption–desorption isotherm curves obtained at 77 K and (b, d) pore size distribution diagrams based on the DFT method of MOP, MOPN-PAA, MOPN-ZnPAA, and ZnPAA.

π – π stacked networks, and interpenetrated networks, which can be the factors of the reduced surface area.^{26,27} We speculate that the nanosizes of MOPN-PAA1 can enhance the degree of networking because of the facilitated diffusion of building blocks in the networking process. In addition, the appropriate existence of PAA in the networks can block the π – π stacking or interpenetration of networks. Thus, we think that these factors induced the increased surface areas and microporosity of MOPN-PAA1, compared with those of MOP. In the cases of MOPN-PAA2 and MOPN-PAA3, surface areas decreased to 523 and 377 m^2/g with micropore volumes of 0.13 and 0.10 cm^3/g , respectively, due to the increased amount of nonporous PAA (Figure 4a, b and Table S1). Considering the nonporous feature of PAA (surface area: 14 m^2/g , V_{mic} : 0 cm^3/g), the high surface areas of MOPN-PAAs mainly originate from the micropores of MOPN.

The difference in porosity and surface areas between MOPN-ZnPAA and ZnPAA was quite distinct (Figure 4c, d). First, the MOPN-ZnPAA showed an enhanced surface area of 669 m^2/g and microporosity (V_{mic} : 0.15 cm^3/g), compared with those of MOPN-PAA2. We speculate that the coordination of zinc ions to carboxylate groups of PAA in MOPN-PAA induced the rigidized chain structure of ZnPAA (Figure 2), hindering the nonporous packing of PAA chains with a resultant increase in the surface area and microporosity of MOPN-ZnPAA, compared with those of MOPN-PAA2. In comparison, while the ZnPAA showed poor microporosity and a reduced surface area of 326 m^2/g , it showed mesoporosity with a pore size of 5–35 nm (Figure 4c, d). We speculate that the poor microporosity of ZnPAA indicates its compact chain structure. Instead, the observed mesoporosity of ZnPAA might result from the packing of rigidized ZnPAA chains.²⁰

The chemical structures of MOP, MOPN-PAA, MOPN-ZnPAA, and ZnPAA were characterized by infrared absorption (IR) spectroscopy (Figure 5a). The IR spectrum of MOP without PAA showed two main peaks at 1505 and 820 cm^{-1} ,

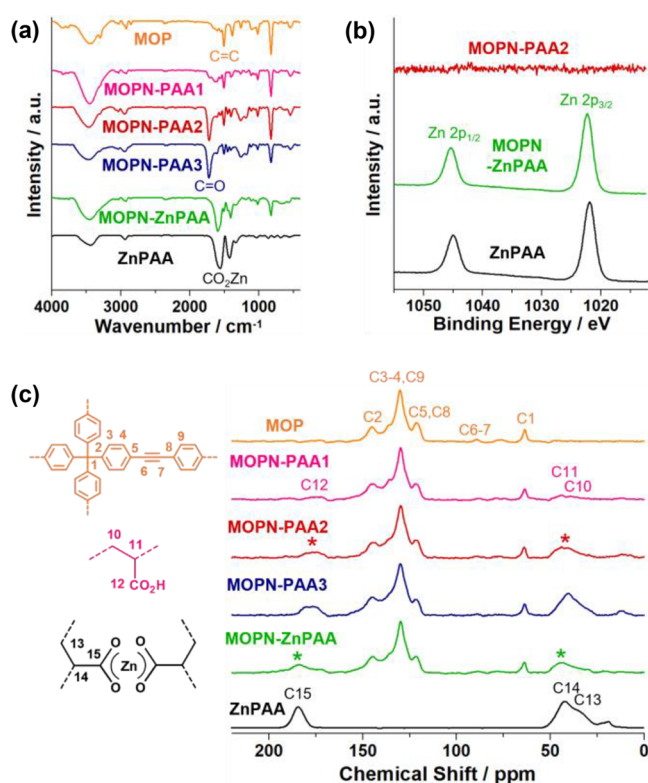


Figure 5. (a) IR spectra of MOP, MOPN-PAA, MOPN-ZnPAA, and ZnPAA. (b) XPS Zn 2p orbital spectra of MOPN-PAA2, MOPN-ZnPAA, and ZnPAA. (c) Solid-state ^{13}C NMR spectra of MOP, MOPN-PAA, MOPN-ZnPAA, and ZnPAA.

corresponding to aromatic C=C and C–H vibrations, respectively, and matching with those of MOPs in the literature.²⁸ In the IR spectrum of MOPN-PAA1, new peaks appeared at 1725 and 1263–1174 cm^{-1} , corresponding to C=O and C–O vibrations of PAA in the MOPN-PAA1, respectively. The relative intensities of PAA peaks increased in the IR spectra of MOPN-PAA2 and MOPN-PAA3, implying the increased amounts of PAA. According to elemental analysis, the contents of PAA in MOPN-PAA1, MOPN-PAA2, and MOPN-PAA3 were analyzed to be 8.0, 19.5, and 29.6%, respectively. In the case of MOPN-ZnPAA, a key vibration peak of coordinated carboxylate moieties was observed at 1560 cm^{-1} , matching well with the vibration peaks of ZnPAA and indicating that the zinc ions were well coordinated to the PAA in the MOPN-PAA2. In the X-ray photoelectron spectroscopy (XPS) of MOPN-ZnPAA, Zn 2p_{1/2} and 2p_{3/2} orbital peaks appeared at 1045.3 and 1022.3 eV, matching well with the control ZnPAA materials and indicating clearly that zinc ions were successfully coordinated to the PAA in the MOPN-PAA2 (Figure 5b).

A solid-state ^{13}C nuclear magnetic resonance (NMR) spectrum of MOP showed the benzylic carbon and alkyne ^{13}C peaks at 64 and 80–90 ppm, respectively (Figure 5c). In addition, aromatic ^{13}C peaks appeared at 121, 130, 136, and 145 ppm, matching well with MOPs prepared in the literature.²⁸ In comparison, new ^{13}C peaks appeared at 35–50 and 177 ppm in the ^{13}C NMR spectrum of MOPN-PAA1, corresponding to the aliphatic and carboxylic acid moieties of PAA. The relative intensities of these PAA peaks significantly increased in the ^{13}C NMR spectra of MOPN-PAA2 and MOPN-PAA3, compared with those of MOPN-PAA1. The

^{13}C peaks of carbonyl and aliphatic groups of PAA in the ^{13}C NMR spectrum of MOPN-ZnPAA shifted to 184 and 27–50 ppm, respectively, indicating the zinc coordination to PAA and matching with those of ZnPAA.

The zinc content in the MOPN-ZnPAA was analyzed to be 2.16 mmol/g by inductively coupled plasma-atomic emission spectroscopy (ICP-AES). Thermogravimetric analysis (TGA) showed that MOPN-ZnPAA is thermally stable up to 402 °C (Figure S4).

Considering the nanoparticulate feature (average diameter of 30 nm), a high surface area (669 m^2/g), and thermal stability of MOPN-ZnPAA, we studied its catalytic performance in the ring-opening polymerization of ϵ -CL to PCL (Figure 6a and Table 1). Due to the nanoparticulate feature,

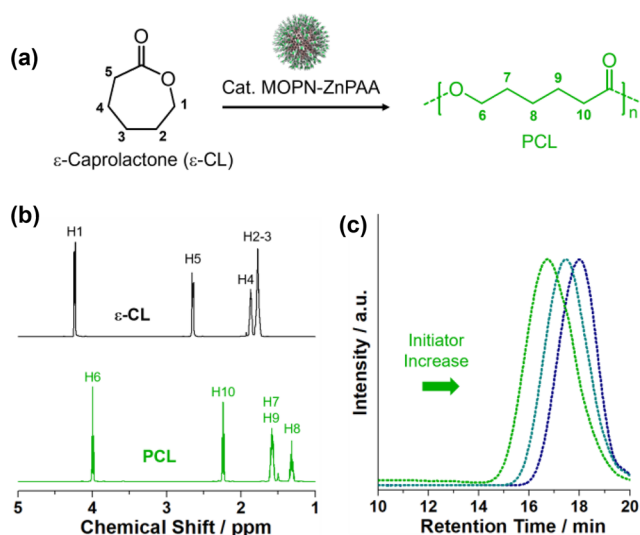


Figure 6. (a) MOPN-ZnPAA catalyzed polymerization of ϵ -caprolactone (ϵ -CL) to polycaprolactone (PCL). (b) ^1H NMR spectrum of ϵ -CL and PCL. (c) GPC chromatograms of PCLs depending on the amount of initiator (4.51 mmol ϵ -CL as a monomer, 45.1 (green), 60.2 (teal), and 180 μmol (dark blue) of H_2O as an initiator).

the MOPN-ZnPAA was well dispersed in the monomer, ϵ -CL. Thus, neat ϵ -CL was used as a reaction medium without any additional solvent. Water was used as an initiator of polymerization. Through scanning amounts of catalysts and initiators, reaction time, and reaction temperature, reaction conditions were optimized. When 1.00 mol % Zn in MOPN-ZnPAA was used at 120 °C for 24 h, PCL (M_n : 18 700, PDI: 1.71) was obtained with a high isolated yield of 96% (Entry 4 in Table 1). While ^1H NMR peaks of ϵ -CL appeared at 4.24 ($-\text{CH}_2\text{O}-$), 2.64 ($-\text{CH}_2\text{CO}_2-$), 1.87 ($-\text{CH}_2\text{CH}_2\text{CH}_2-$), and 1.78 ($-\text{CH}_2\text{CH}_2\text{CH}_2-$) ppm, those of PCL shifted to 3.99 ($-\text{CH}_2\text{O}-$), 2.24 ($-\text{CH}_2\text{CO}_2-$), 1.58 ($-\text{CH}_2\text{CH}_2\text{CH}_2-$), and 1.32 ($-\text{CH}_2\text{CH}_2\text{CH}_2-$) ppm (Figure 6b), indicating the successful formation of PCL.²⁹ Similarly, while ^{13}C NMR peaks of ϵ -CL appeared at 176.2 ($-\text{CO}_2-$), 69.3 ($-\text{CH}_2\text{O}-$), 34.6 ($-\text{CH}_2\text{CO}_2-$), 29.3 ($-\text{CH}_2\text{CH}_2\text{CH}_2-$), 29.0 ($-\text{CH}_2\text{CH}_2\text{CH}_2-$), and 23.0 ($-\text{CH}_2\text{CH}_2\text{CH}_2-$) ppm, those of PCL shifted to 173.6 ($-\text{CO}_2-$), 64.2 ($-\text{CH}_2\text{O}-$), 34.1 ($-\text{CH}_2\text{CO}_2-$), 28.4 ($-\text{CH}_2\text{CH}_2\text{CH}_2-$), 25.5 ($-\text{CH}_2\text{CH}_2\text{CH}_2-$), and 24.6 ($-\text{CH}_2\text{CH}_2\text{CH}_2-$) ppm (Figure S5). In the absence of catalysts, no conversion of ϵ -CL was observed (Entry 1 in Table 1).

Table 1. Ring-Opening Polymerization of ϵ -Caprolactone to Polycaprolactone by MOPN-ZnPAA^a

entry	Cat. ^b	Zn (mol %)	time (h)	M_n	PDI	yield ^c (%)
1			24			0
2	ZnPAA	1.00	24	14 500	1.68	95
3 ^d	ZnPAA	1.00	24			0
4	1	1.00	24	18 700	1.71	96
5	1	0.500	24	7900	1.48	92
6	1	0.250	24	7200	1.42	91
7	1	0.125	24	5700	1.21	82
8 ^e	1	1.00	24	14 600	1.61	94
9 ^f	1	1.00	24	2700	1.15	47
10	1	1.00	12	13 700	1.43	87
11	1	1.00	6	9100	1.18	73
12	1	1.00	3	7100	1.10	50
13 ^g	1	1.00	24	11 500	1.55	95
14 ^h	1	1.00	24	8700	1.40	81
15 ⁱ	1	1.00	24	13 700	1.45	93
16 ^j	1	1.00	24	14 700	1.49	91
17 ^k	1	1.00	24	16 000	1.46	88
18 ^l	1	1.00	24	14 500	1.53	91

^aReaction conditions: ϵ -caprolactone (4.51 mmol), MOPN-ZnPAA (0.125–1.00 mol % Zn, 2.16 mmol Zn/g), initiator (H_2O , 45.1 μmol), and 120 °C. ^bMOPN-ZnPAA is indicated by 1. ^cIsolated yields. ^dThe catalyst recovered from entry 2 was used. ^eReaction temperature of 150 °C. ^fReaction temperature of 90 °C. ^g0.2 μmol H_2O was used as an initiator. ^h180 μmol H_2O was used as an initiator. ⁱThe catalyst recovered from entry 4 was used. ^jThe catalyst recovered from entry 15 was used. ^kThe catalyst recovered from entry 16 was used. ^lThe catalyst recovered from entry 17 was used.

When the amount of MOPN-ZnPAA was decreased from 1.00 mol % to 0.500, 0.250, and 0.125 mol % Zn, isolated yields of PCL gradually decreased from 96% to 92, 91, and 82% with a significant decrease in M_n from 18 700 to 7900, 7200, and 5700, respectively (Entries 4–7 in Table 1). When the reaction temperature was decreased from 120 to 90 °C, isolated yields of PCL sharply decreased from 96 to 47% with a decrease in M_n from 18 700 to 2700 (Entries 4 and 8–9 in Table 1), due to increased viscosity of reaction media (neat ϵ -CL) at a lower temperature. When the reaction time was decreased from 24 to 12, 6, and 3 h, isolated yields of PCL gradually decreased from 96 to 87, 73, and 50% with a decrease in M_n from 18 700 to 13 700, 9100, and 7100, respectively (Entries 4 and 10–12 in Table 1). With 1.00 mol % MOPN-ZnPAA, the length of PCL chains could be controlled by changing the amount of an initiator (Figure 6c). As the amount of an initiator, water, was increased from 45.1 μmol to 90.2 and 180 μmol , M_n values decreased from 18 700 to 11 500 and 8700, respectively, due to an increase in the number of polymer chains (Entries 13–14 in Table 1).³⁰ Thus, 1.00 mol % MOPN-ZnPAA, 1.00 mol % initiator, 120 °C, and 24 h were determined as optimized reaction conditions for the ring-opening polymerization of ϵ -CL to PCL.

While a control system, 1.00 mol % ZnPAA, showed significant catalytic performance for ring-opening polymerization of ϵ -CL with a 95% isolated yield of PCL (M_n : 14 500), it could not be recycled (Entries 2–3 in Table 1). In comparison, 1.00 mol % MOPN-ZnPAA showed excellent recyclability, maintaining the 88–93% isolated yields of PCL and M_n values of 13 700–16 000 in the successive four recycling reactions (Entries 15–18 in Table 1). SEM and XPS analysis of MOPN-ZnPAA recovered after recycling tests

showed that original nanoparticulated morphologies and chemical structure were completely maintained (Figure S6). In addition, ICP-AES analysis indicated that 99.4% zinc was retained in the recovered MOPN-ZnPAA.

In conclusion, an in situ synthetic approach has been developed for the engineering of nanoplatforms. The addition of PAA to the reaction mixture for Sonogashira coupling-based MOPs induced the size-controlled formation of MOP nanoparticles. Simultaneously, PAA chains were in situ entrapped into MOP networks to form MOPN with PAA anchoring groups. The reaction of MOPN-PAA with zinc ions resulted in the formation of a nanoscaled MOPN-ZnPAA catalyst. Heating of neat ϵ -CL in the presence of 1.00 mol % MOPN-ZnPAA and 1.00 mol % water resulted in the formation of PCL. Moreover, MOPN-ZnPAA could be recycled with the retention of catalytic performance in five successive runs. Compared with the conventional engineering of heterogeneous nanocatalysts through the stepwise synthesis of nanosupports and introduction of anchoring groups, a new synthetic approach in this work showed simultaneous trap of anchoring groups into MOP networks during kinetically controlled growth of MOP nanoparticles. We believe that an efficient and new synthetic approach of this work can be applied to the engineering of various heterogeneous nanocatalysts.

■ ASSOCIATED CONTENT

SI Supporting Information

The Supporting Information is available free of charge at <https://pubs.acs.org/doi/10.1021/acsanm.2c03480>.

Synthetic and experimental procedures and additional characterization data of MOPN-PAA, MOPN-ZnPAA, and recycled MOPN-ZnPAA (PDF)

■ AUTHOR INFORMATION

Corresponding Author

Seung Uk Son – Department of Chemistry, Sungkyunkwan University, Suwon 16419, Korea; orcid.org/0000-0002-4779-9302; Email: sson@skku.edu

Authors

Jong Doo Lee – Department of Chemistry, Sungkyunkwan University, Suwon 16419, Korea

Yoon-Joo Ko – Laboratory of Nuclear Magnetic Resonance, The National Center for Inter-University Research Facilities (NCIRF), Seoul National University, Seoul 08826, Korea

Sang Moon Lee – Korea Basic Science Institute, Daejeon 34133, Korea

Hae Jin Kim – Korea Basic Science Institute, Daejeon 34133, Korea; orcid.org/0000-0002-1960-0650

Complete contact information is available at: <https://pubs.acs.org/doi/10.1021/acsanm.2c03480>

Notes

The authors declare no competing financial interest.

■ ACKNOWLEDGMENTS

This work was supported by the National Research Foundation of Korea (NRF) grant (2020R1A2C2004310) and “Carbon Upcycling Project for Platform Chemicals” (2022M3J3A1046019) funded by the Ministry of Science and ICT, Republic of Korea.

■ REFERENCES

- (1) Baig, N.; Kammakakam, I.; Falath, W. Nanomaterials: A Review of Synthesis Methods, Properties, Recent Progress, and Challenges. *Mater. Adv.* **2021**, *2*, 1821–1871.
- (2) Mitchell, S.; Qin, R.; Zheng, N.; Pérez-Ramírez, J. Nanoscale Engineering of Catalytic Materials for Sustainable Technologies. *Nat. Nanotechnol.* **2021**, *16*, 129–139.
- (3) Shifrina, Z. B.; Matveeva, V. G.; Bronstein, L. M. Role of Polymer Structures in Catalysis by Transition Metal and Metal Oxide Nanoparticle Composites. *Chem. Rev.* **2020**, *120*, 1350–1396.
- (4) Singh, D. K.; Jagannathan, R.; Khandelwal, P.; Abraham, P. M.; Poddar, P. In Situ Synthesis and Surface Functionalization of Gold Nanoparticles with Curcumin and Their Antioxidant Properties: An Experimental and Density Functional Theory Investigation. *Nanoscale* **2013**, *5*, 1882–1893.
- (5) Dalod, A. R. M.; Grendal, O. G.; Skjærø, S. L.; Inzani, K.; Selbach, S. M.; Henriksen, L.; van Beek, W.; Grande, T.; Einarsrud, M.-A. Controlling Oriented Attachment and In Situ Functionalization of TiO₂ Nanoparticles During Hydrothermal Synthesis with APES. *J. Phys. Chem. C* **2017**, *121*, 11897–11906.
- (6) Cho, K.; Kang, C. W.; Ryu, S. H.; Jang, J. Y.; Son, S. U. The Rise of Morphology-Engineered Microporous Organic Polymers (MEMOPs): Synthesis and Benefits. *J. Mater. Chem. A* **2022**, *10*, 6950–6964.
- (7) Imam, H. T.; Marr, P. C.; Marr, A. C. Enzyme Entrapment, Biocatalyst Immobilization without Covalent Attachment. *Green. Chem.* **2021**, *23*, 4980–5005.
- (8) Chen, G.; Zhao, Y.; Shang, L.; Waterhouse, G. I. N.; Kang, X.; Wu, L.-Z.; Tung, C.-H.; Zhang, T. Recent Advances in the Synthesis, Characterization and Application of Zn²⁺-containing Heterogeneous Catalysts. *Adv. Sci.* **2016**, *3*, 1500424.
- (9) Bystrzanowska, M.; Petkov, P.; Tobiszewski, M. Ranking of Heterogeneous Catalysts Metals by Their Greenness. *ACS Sustainable Chem. Eng.* **2019**, *7*, 18434–18443.
- (10) Abbina, S.; Du, G. Zinc-Catalyzed Highly Isoselective Ring Opening Polymerization of rac-Lactide. *ACS Macro Lett.* **2014**, *3*, 689–692.
- (11) Mercadé, E.; Zangrando, E.; Claver, C.; Godard, C. Robust Zinc Complexes That Contain Pyrrolidine-Based Ligands as Recyclable Catalysts for the Synthesis of Cyclic Carbonates from Carbon Dioxide and Epoxides. *ChemCatChem* **2016**, *8*, 234–243.
- (12) Wang, W.; Li, C.; Yan, L.; Wang, Y.; Jiang, M.; Ding, Y. Ionic Liquid/Zn-PPH₃ Integrated Porous Organic Polymers Featuring Multifunctional Sites: Highly Active Heterogeneous Catalyst for Cooperative Conversion of CO₂ to Cyclic Carbonates. *ACS Catal.* **2016**, *6*, 6091–6100.
- (13) Patel, P.; Patel, U.; Parmar, B.; Dadhania, A.; Suresh, E. Regioselective Ring-Opening of Spiro-Epoxyoxindoles by a Dual Ligand Zinc-Based Metal-Organic Framework as an Efficient Heterogeneous Catalyst. *ACS Appl. Nano Mater.* **2022**, *5*, 3712–3721.
- (14) Chapman, A. M.; Keyworth, C.; Kember, M. R.; Lennox, A. J. J.; Williams, C. K. Adding Value to Power Station Captured CO₂: Tolerant Zn and Mg Homogeneous Catalysts for Polycarbonate Polyol Production. *ACS Catal.* **2015**, *5*, 1581–1588.
- (15) Labet, M.; Thielemans, W. Synthesis of Polycaprolactone: A Review. *Chem. Soc. Rev.* **2009**, *38*, 3484–3504.
- (16) Gruszka, W.; Garden, J. A. Advances in Heterometallic Ring-Opening (Co)Polymerisation Catalysis. *Nat. Commun.* **2021**, *12*, 3252.
- (17) Liu, H.; Khononov, M.; Fridman, N.; Tamm, M.; Eisen, M. S. (Benz)Imidazolin-2-iminato Aluminum, Zinc, and Magnesium Complexes and Their Applications in Ring Opening Polymerization of ϵ -Caprolactone. *Inorg. Chem.* **2019**, *58*, 13426–13439.
- (18) Pérez, Y.; del Hierro, I.; Zazo, L.; Fernández-Galán, R.; Fajardo, M. The Catalytic Performance of Metal Complexes Immobilized on SBA-15 in the Ring Opening Polymerization of ϵ -Caprolactone with Different Metals (Ti, Al, Zn and Mg) and Immobilization Procedures. *Dalton Trans.* **2015**, *44*, 4088–4101.

(19) Howard, I. C.; Hammond, C.; Buchard, A. Polymer-Supported Metal Catalysts for the Heterogeneous Polymerisation of Lactones. *Polym. Chem.* **2019**, *10*, 5894–5904.

(20) Tan, T.; Park, S.-Y. Poly(acrylic acid) Hydrogel Microspheres for a Metal-Ion Sensor. *ACS Sens.* **2021**, *6*, 1039–1048.

(21) Patra, A.; Koenen, J.-M.; Scherf, U. Fluorescent Nanoparticles Based on a Microporous Organic Polymer Network: Fabrication and Efficient Energy Transfer to Surface-Bound Dyes. *Chem. Commun.* **2011**, *47*, 9612–9614.

(22) Wu, K.; Guo, J.; Wang, C. Dispersible and Discrete Metalloporphyrin-Based CMP Nanoparticles Enabling Colorimetric Detection and Quantitation of Gaseous SO₂. *Chem. Commun.* **2014**, *50*, 695–697.

(23) Wu, X.; Li, H.; Xu, B.; Tong, H.; Wang, L. Solution-Dispersed Porous Hyperbranched Conjugated Polymer Nanoparticles for Fluorescent Sensing of TNT with Enhanced Sensitivity. *Polym. Chem.* **2014**, *5*, 4521–4525.

(24) Ma, B. C.; Ghasimi, S.; Landfester, K.; Vilela, F.; Zhang, K. A. I. Conjugated Microporous Polymer Nanoparticles with Enhanced Dispersibility and Water Compatibility for Photocatalytic Applications. *J. Mater. Chem. A* **2015**, *3*, 16064–16071.

(25) Lee, D. H.; Ko, K. C.; Ko, J. H.; Kang, S. Y.; Lee, S. M.; Kim, H. J.; Ko, Y.-J.; Lee, J. Y.; Son, S. U. In Situ Water-Compatible Polymer Entrapment: A Strategy for Transferring Superhydrophobic Microporous Organic Polymers to Water. *ACS Macro Lett.* **2018**, *7*, 651–655.

(26) Kim, B.; Park, N.; Lee, S. M.; Kim, H. J.; Son, S. U. Insights into the Low Surface Area of Conjugated Microporous Polymers and Methodological Suggestion for the Enhanced of Porosity. *Polym. Chem.* **2015**, *6*, 7363–7367.

(27) Ben, T.; Ren, H.; Ma, S.; Cao, D.; Lan, J.; Jing, X.; Wang, W.; Xu, J.; Deng, F.; Simmons, J. M.; et al. Targeted Synthesis of a Porous Aromatic Framework with High Stability and Exceptionally High Surface Area. *Angew. Chem., Int. Ed.* **2009**, *48*, 9457–9460.

(28) Jang, J. Y.; Duong, H. T. T.; Lee, S. M.; Kim, H. J.; Ko, Y.-J.; Jeong, J. H.; Lee, D. S.; Thambi, T.; Son, S. U. Folate Decorated Hollow Spheres of Microporous Organic Networks as Drug Delivery Materials. *Chem. Commun.* **2018**, *54*, 3652–3655.

(29) Tarnacka, M.; Dzienia, A.; Maksym, P.; Talik, A.; Zieba, A.; Bielas, R.; Kaminski, K.; Paluch, M. Highly Efficient ROP Polymerization of *ε*-Caprolactone Catalyzed by Nanoporous Alumina Membranes. How the Confinement Affects the Progress and Product of ROP Reaction. *Macromolecules* **2018**, *51*, 4588–4597.

(30) Baez, J. E.; Martinez-Richa, A.; Marcos-Fernandez, A. One-Step Route to α -Hydroxyl- ω -(carboxylic Acid) Polylactones Using Catalysis by Decamolybdate Anion. *Macromolecules* **2005**, *38*, 1599–1608.

Recommended by ACS

Catalysts Based on Porous Polyaromatic Frameworks for Deep Oxidative Desulfurization of Model Fuel in Biphasic Conditions

Leonid A. Kulikov, Eduard A. Karakhanov, *et al.*

OCTOBER 21, 2019
INDUSTRIAL & ENGINEERING CHEMISTRY RESEARCH

READ 

Synthesis of Poly(phenylene ethynylene) Using an Easily Recyclable Pd-Functionalized Magnetite Nanoparticle Catalyst

Amaury De Cattelle, Guy Koeckelberghs, *et al.*

MARCH 05, 2020
MACROMOLECULES

READ 

Porous Organic Polymers Containing Active Metal Centers for Suzuki–Miyaura Heterocoupling Reactions

Noelia Esteban, Jesús A. Miguel, *et al.*

DECEMBER 11, 2020
ACS APPLIED MATERIALS & INTERFACES

READ 

Highly Selective Oxidation of Styrene to Styrene Oxide over a Tetraphenylporphyrin-Bridged Silsesquioxane-Based Hybrid Porous Polymer

Chenyu Sun and Hongzhi Liu

JUNE 30, 2022
ACS APPLIED POLYMER MATERIALS

READ 

Get More Suggestions >